Since January 2020 Elsevier has created a COVID-19 resource centre with free information in English and Mandarin on the novel coronavirus COVID-19. The COVID-19 resource centre is hosted on Elsevier Connect, the company's public news and information website.

Current Problems in Diagnostic Radiology 52 (2023) 117–124

Current Problems in Diagnostic Radiology

journal homepage: www.cpdrjournal.com

Role of MRI in the Evaluation of Pulmonary Sequel Following COVID-19 Acute Respiratory Distress Syndrome (ARDS)

Mandeep Garg, MD, FRCR[a,*], Saurav Lamicchane, MD[a], Muniraju Maralakunte, MD[a], Uma Debi, MD[a], Sahajal Dhooria, DM[b], Inderpaul Sehgal, DM[b], Nidhi Prabhakar, MD[a], Manavjit Singh Sandhu, MD[a]

[a] *Deptt. of Radiodiagnosis & Imaging, PGIMER, Chandigarh, India*
[b] *Deptt. of Pulmonary Medicine, PGIMER, Chandigarh, India*

To evaluate the role of magnetic resonance imaging (MRI) chest as an alternative modality to CT chest for follow-up of patients recovered from severe COVID-19 acute respiratory distress syndrome (ARDS). A total of 25 subjects (16 [64%] men; mean age 54.84 years ± 12.35) who survived COVID-19 ARDS and fulfilled the inclusion criteria were enrolled prospectively. All the patients underwent CT and MRI chest (on the same day) at 6-weeks after discharge. MRI chest was acquired on 1.5T MRI using HASTE, BLADE, VIBE, STIR, and TRUFI sequences and evaluated for recognition of GGOs, consolidation, reticulations/septal thickening, parenchymal bands, and bronchial dilatation with CT chest as the gold standard. The differences were assessed by independent-sample *t*-test and Mann-Whitney *U* test. *P*-value of less than 0.05 was taken significant. There was a strong agreement (k = 0.8-1, $P<0.01$) between CT and MRI chest. On CT, the common manifestations were: GGOs (n=24, 96%), septal thickening/reticulations (n=24, 96%), bronchial dilatation (n=16, 64%), parenchymal bands (n=14, 56%), pleural thickening (n=8, 32%), consolidation (n=4, 16%) and crazy-paving (n=4, 16%). T2W HASTE, T2W BLADE, and T1 VIBE sequences showed 100% (95% CI, 40-100) sensitivity and 100% (95% CI, 3-100) specificity for detecting GGOs, septal thickening/reticulations, pleural thickening, consolidation, and crazy-paving. The overall sensitivity of MRI for detection of bronchial dilatation and parenchymal bands were 88.9% (95% CI, 77-100) and 92.9% (95% CI, 66-100), respectively; and specificity was 100% (95% CI, 29-100) for both findings. MRI chest, being radiation-free imaging modality can act as an alternative to CT chest in the evaluation of lung changes in patients recovered from COVID-19 pneumonia.

Introduction

A significant number of patients who recovered from COVID-19 pneumonia continue to have lingering illnesses even in their post-recovery phase. The reported prevalence of the persistent COVID-19 symptoms and its complications is 1 in 5 COVID-19 survivors at 5 weeks or longer[1] with the lungs being the most involved organ. Decreased diffusion capacity was the most prevalent (0.66, CI 0.31-0.94, $P<0.01$, I2 = 82%) pulmonary function alteration reported by a meta-analysis on post-COVID subjects, with reduction directly associated with clinical severity of the acute COVID-19 pneumonia.[2] A prospective study from China reported persistence of 1 or more pulmonary computed tomography (CT) findings in more than 60% of post-COVID-19 subjects 6 months following infection.[3] Increased age, severe acute COVID-19 pneumonia, deranged inflammatory markers, diffuse pulmonary involvement on imaging, presence of multiple co-morbidities, ICU admission, the requirement of mechanical ventilation, and presence of 5 or more symptoms at acute presentation were associated with a significant pulmonary or systemic sequel following COVID-19 pneumonia.[4] Imaging plays a central role in evaluating the pulmonary sequel in such high-risk group patients.

CT chest is an invaluable tool utilized frequently in the diagnosis and management of acute COVID-19 as well as in the follow-up of the pulmonary sequel in COVID-19 survivors.[5-7] The natural course of the pulmonary findings is varied, with the majority of the findings in mild to moderate disease seen to resolve over time. Nevertheless, a significant number of subjects are shown to have persistent ground-glass opacities (GGOs) and/or interstitial thickening, and fibrotic-like lesions in 27% (n= 31/114) and 35% (n= 40/114) of the severe COVID-19 pneumonia survivors at 6 months and 1-year follow-up.[3,8] Currently, there is a lack of true understanding of the nature of the pulmonary manifestations on CT imaging.[4] Chest care experts advise for follow-up CT chest imaging in the high-risk subjects to correlate with clinical parameters and pulmonary function test (PFT).[4,9] Such patients often need repeat CT examinations to monitor the disease progression, and this can lead to a higher cumulative dose to the patients and to the community; considering the enormous burden of the disease.

Magnetic resonance imaging (MRI) chest can be a good alternative imaging modality to CT chest for follow-up of the post-COVID-19 patients, as it doesn't impart ionizing radiation.[10-12] Several authors have studied the diagnostic accuracy of MRI chest, and lately, few studies have shown that the detection rate of MRI chest is comparable to that of CT chest in acute COVID-19 pneumonia, and other chest conditions.[10,11,13,14] We evaluated the diagnostic performance of 1.5T MRI chest, done at 6 weeks of discharge in patients recovered from COVID-19 acute respiratory distress syndrome (ARDS); taking CT chest as a reference standard.

Mandeep Garg and Saurav Lamicchane share first authorship equally.

*Reprint requests: Mandeep Garg, MD, FRCR, Deptt. of Radiodiagnosis and Imaging, PGIMER. Chandigarh. Sector-12, India.
E-mail address: gargmandeep@hotmail.com (M. Garg).

https://doi.org/10.1067/j.cpradiol.2022.09.001
0363-0188/

METHODS

Study design and participants

Institutional ethics committee (IEC) gave the approval for this prospective study. Written informed consent was obtained from all the study participants. Patient confidentiality was ensured according to the HIPPA guidelines.

A total of 25 subjects of severe COVID-19 pneumonia and ARDS were enrolled for the study who were discharged from the hospital between December 2020 to June 2021. A diagnosis of severe COVID-19 pneumonia was based on the WHO's interim guidance diagnostic criteria,[15] and the Berlin definition was used for ARDS.[16] All patients had laboratory confirmation of SARS-CoV-2 using real-time reverse-transcription polymerase chain reaction (RT-PCR) at admission. The discharge criteria were based on remission of acute respiratory distress symptoms, and/or negative RT-PCR before discharge (on 2 occasions, performed 24 hours apart).[17]

The patients meeting the above inclusion criteria were called for follow-up at 6 weeks of discharge from the hospital. Patients who refused to give consent and those with contraindication for MRI chest (claustrophobic, with severe dyspnea and with metallic cardiac pacemakers) were excluded from the study (Fig 1). Spirometry and a 6-minute walk test (6-MWT) were performed for each patient, and the findings were recorded. The patients underwent non-enhanced CT chest followed by MRI chest on the same day. The time taken for MRI chest was recorded for each patient. The clinical details such as age, gender, co-morbidities, the severity of the disease, duration of the hospital stay, and treatment details were recorded from the available medical records.

CT chest protocol

CT chest imaging was performed on a third-generation dual-source CT 128 slice scannerSomatom Definition Flash (Siemens Healthcare, Forchheim, Germany) or CT 256 Slice scanner (Philips Brilliance iCT). Non-enhanced CT chest was acquired from the thoracic inlet to the diaphragm with the patient in the supine position. The following acquisition parameters were used: tube voltage of 120 kVp and detector collimation width of 128 × 0.6 mm or 256 × 0.6 mm. The helical dataset for the chest was acquired with 10 mm thick sections at 10 mm increment with tube current regulated by an automated exposure control (AEC) system. Images reconstructed into 1 mm sections at 1 mm increment using 2 different reconstruction kernels (B70 ultra-sharp for lung window and B30 smooth for mediastinal window) using regular filter back projection.

Thorax MRI protocol

MRI scan was done on a 1.5 Tesla MR unit (MAGNETOM AERA; Siemens Medical Solutions, Malvern, Pa) with the patient in the supine position using a body coil. The center of the coil was positioned at the mid-sternum. To minimize dynamic artifacts associated with respiratory movements, the RF coil was fixed. Imaging parameters were as follows: T2-weighted HASTE (Half-Fourier Acquisition Single-shot Turbo Spin-Echo) Coronal [breath-hold], TR/TE (time to repitition/time to echo) ~1000/90 ms, FOV of 35 cm, slice thickness of 6 mm; T2-weighted BLADE (proprietary name for Periodically Rotated Overlapping Parallel Lines with Enhanced Reconstruction [PROPELLER]) axial (respiratory-triggered), TR/TE ~2500/118 ms, FOV of 32 cm, slice thickness of 5 mm; T1-weighted 3D VIBE (Volume Interpolated Breath-hold Examination) axial [breath-hold], TR/TE ~2.6/0.94 ms, FOV of 35 cm, slice thickness of 2.2 mm; T2-weighted STIR (Short Tau Inversion Recovery) coronal [respiratory-triggered] TR/TE ~500/39 ms, FOV of 32 cm, slice thickness of 5 mm; T2-weighted TRUFI (True Fast Imaging with Steady State Free Precession) coronal [free-breathing], with TR/TE ~448/144 ms, FOV of 32 cm, slice thickness of 5 mm.

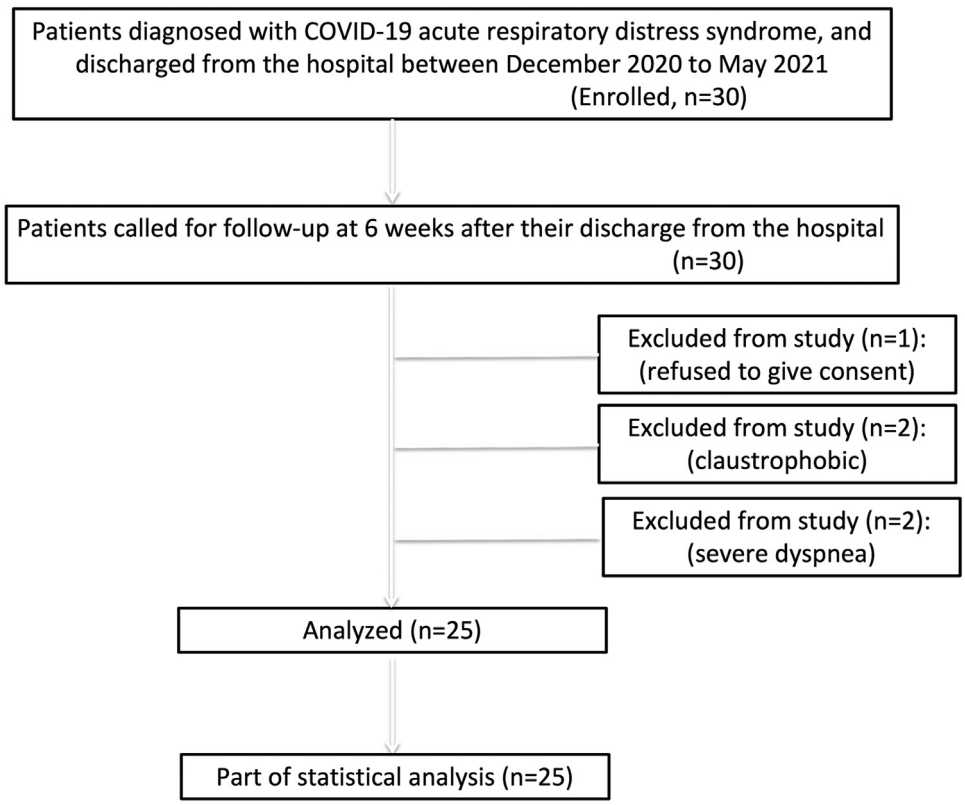

FIG 1. Flowchart depicting the recruitment process of the study participants, inclusion and exclusion criteria and the included subjects.

Image analysis

CT chest was considered the gold standard in this study. The MRI and CT images of all patients were evaluated independently by 2 thoracic radiologists (M.G. and U.D., with 20 and 10 years of experience, respectively). Both the reviewers were blinded to the clinical details of the patients. All the images were deidentified, and randomization of CT and MRI images was done. The discrepancy between reviewers was resolved by consensus reading in the third session. To describe lung findings, the Fleischner Society Glossary[18] terms were used: GGOs, consolidation, reticulations, inter and intralobular septal thickening, crazy-paving and parenchymal bands. However, instead of traction bronchiectasis and bronchiolectasis, we used the terms bronchial dilatation and subpleural multicystic changes; as traction bronchiectasis and bronchiolectasis denotes irreversible changes and bronchial dilatation found at 6 weeks may be a reversible finding and not due to true fibrosis.

Since there are no separate terms to describe the pulmonary parenchymal findings on MRI, the same CT terms were utilized for interpretation of MRI chest abnormalities.

Statistical Analysis

Statistical analysis was done using the R-software package (version 3.6.3; R Foundation for Statistical Computing, Vienna, Austria). The quantitative variables were presented as median and mean ± standard deviation for descriptive statistics, and categorical variables were stated as frequencies and percentages. The chi-square test was used for the comparison of categorical variables. A value of $P < 0.05$ was accepted as statistically significant. The sensitivity, specificity, positive predictive value, and negative predictive value of MRI findings were calculated for each patient, with CT chest imaging as a reference modality. The independent samples *t*-test was used to compare continuous variables with normal distribution and the Mann-Whitney *U* test for the comparison of continuous variables that are not normally distributed. Cohen's Kappa coefficient (*k*) assessed coherence between 2 observers for pulmonary findings.

RESULTS

Demographic and clinical data (Table 1)

(Table 1) From a total of 30 enrolled patients, 5 patients were excluded from the study - 1 refused to give consent for MRI and 2 patients each had claustrophobia and severe dyspnea. Finally, twenty-five participants (n=9 female and n=16 male) were included in the study with a mean age of 54.84 ± 12.35 (SD) years. The major symptoms of the participants at the time of follow-up include: dyspnea (n=25, 100%), fatigue (n=22, 88%) and cough (n=20, 80%). The mean duration of hospital stay during acute disease was 11.84 ± 5.25 days. The mean RT-PCR (negative results) to follow-up CT/MRI interval was 46.72 ± 27.42. Diabetes mellitus (n=19, 76%), hypertension (n=10, 40%), and obesity (n=5, 20%) were the common underlying co-morbidities found in study participants. The mean FVC (% predicted) was 75.71 ± 14.39. The mean FEV1 (% predicted) was 77.23 ± 14.59. The mean FEV1/FVC Ratio (LLN) was 79.06 ± 6.01. The mean distance covered during 6-MWT was 311.02 ± 106.97 meters, and the mean 6-MWT SpO2 was 92.84 ± 4.5%. The mean time taken to complete MRI examination was 11.72 ± 0.39 minutes.

CT findings (Table 2)

(Table 2) On CT, bilateral lung involvement was observed in 24 (96%) study participants, with GGOs (n=24, 96%), septal thickening/reticulations (n=24, 96%) and bronchial dilatation/subpleural multicystic changes (n=16, 64%) being the most common CT abnormalities seen. Other CT findings were: parenchymal bands (n=14, 56%), thickening of the adjacent pleura (n=8, 32%), consolidation (n=4, 16%), and crazy-paving (n=4, 16%). Fourteen (56.0%) participants had a combination of GGOs and reticulations while 3 (16.0%) subjects showed a mixed pattern of GGOs, septal thickening, and consolidation.

TABLE 1.
Demographic and clinical details of the study participants

Basic details	Observations
Total participants (n)	25
Age (y)	54.84 ± 12.35 (Mean ± SD)
Gender	Frequency (%)
Male	16 (64.0%)
Female	9 (36.0%)
Duration of hospital stay (d)	11.84 ± 5.25 (Mean ± SD)
Associated comorbidities	Frequency (%)
Diabetes mellitus	19 (76.0%)
Hypertension	10 (40.0%)
Obesity	5 (20.0%)
Connective Tissue Disorders	2 (8.0%)
Cerebrovascular Accident	1 (4.0%)
RT PCR-CT/MRI interval (d)	46.72 ± 27.42 (Mean ± SD)
Symptoms during follow-up	Frequency (%)
Dyspnea	25 (100.0%)
Fatigue	22 (88.0%)
Cough	20 (80.0%)
Expectoration	3 (12.0%)
Chest pain	2 (8.0%)
mMRC dyspnea scale	Frequency (%)
Grade 1	5 (20.0%)
Grade 2	8 (32.0%)
Grade 3	12 (48.0%)
Grade 4	0 (0%)
6-Min walk test (6-MWT)	(Mean ± SD)
Distance walked (meters)	311.02 ± 106.97
SpO_2 (%)	92.84 ± 4.55
Mean time taken for MRI examination (Min)	11.72 ± 0.39 (Mean ± SD)

mMRC, modified medical research council; SD, standard deviation; SpO_2, saturation of peripheral oxygen.

MRI findings and interobserver analysis (Table 3)

(Table 3) MRI provided diagnostic quality images in all the study participants. GGOs were seen in 24/25 (96%) of subjects with 100% sensitivity (95% CI, 86-100) and 100% specificity (95% CI, 3-100) on T2 HASTE, T2 BLADE, T1 VIBE, and STIR sequences (Fig 2). TRUFI sequence showed GGOs in 20/25 (80%) of subjects with a sensitivity of 83.3% (95 CI, 63-95) and 100% specificity (95% CI, 3-100). Septal thickening and reticulations were seen in 24/25 (96%) of subjects with 100% sensitivity (95% CI, 86-100) and 100% specificity (95% CI, 3-100) on all sequences except for TRUFI (Figs 3 and 4). On TRUFI, 18/25 (72%) subjects showed septal thickening and reticulations; with 75% (95% CI, 53-90) sensitivity and 100% specificity.

Bronchial dilatation/subpleural multicystic changes were seen in 14/25 (56%) of subjects on T2 BLADE and T1 VIBE sequences, with

TABLE 2.
Lung findings at 6-wk follow-up imaging after discharge from hospitalization in patients of COVID-19 acute respiratory distress syndrome (ARDS)

Imaging findings	Frequency (%) on CT chest	Frequency (%) on MRI chest
Ground glass opacities (GGOs)	24 (96.0%)	24 (96.0%)
Septal thickening/reticulations	24 (96.0%)	24 (96.0%)
Bronchial dilatation/subpleural multicystic changes	16 (64.0%)	14 (56.0%)
Parenchymal bands	14 (56.0%)	13 (52.0%)
Pleural thickening	8 (32.0%)	8 (32.0%)
Crazy-paving	4 (16.0%)	4 (16.0%)
Consolidation	4 (16.0%)	4 (16.0%)

TABLE 3
Major lung findings on different MRI sequences

Variable	Total positives	Sensitivity	Specificity	PPV	NPV	Diagnostic accuracy	Kappa	*P* Value
GGOs								
Overall	24 (96.0%)	100.0% (86-100)	100.0% (3-100)	100.0% (86-100)	100.0% (3-100)	100.0% (86-100)	1	<0.001
T2 HASTE	24 (96.0%)	100.0% (86-100)	100.0% (3-100)	100.0% (86-100)	100.0% (3-100)	100.0% (86-100)	1	<0.001
T2 BLADE	24 (96.0%)	100.0% (86-100)	100.0% (3-100)	100.0% (86-100)	100.0% (3-100)	100.0% (86-100)	1	<0.001
T1 VIBE	24 (96.0%)	100.0% (86-100)	100.0% (3-100)	100.0% (86-100)	100.0% (3-100)	100.0% (86-100)	1	<0.001
TRUFI	20 (80.0%)	83.3% (63-95)	100.0% (3-100)	100.0% (83-100)	20.0% (1-72)	84.0% (64-95)	0.29	0.041
STIR	24 (96.0%)	100.0% (86-100)	100.0% (3-100)	100.0% (86-100)	100.0% (3-100)	100.0% (86-100)	1	<0.001
Consolidation								
Overall	4 (16.0%)	100.0% (40-100)	100.0% (84-100)	100.0% (40-100)	100.0% (84-100)	100.0% (86-100)	1	<0.001
T2 HASTE	4 (16.0%)	100.0% (40-100)	100.0% (84-100)	100.0% (40-100)	100.0% (84-100)	100.0% (86-100)	1	<0.001
T2 BLADE	4 (16.0%)	100.0% (40-100)	100.0% (84-100)	100.0% (40-100)	100.0% (84-100)	100.0% (86-100)	1	<0.001
T1 VIBE	4 (16.0%)	100.0% (40-100)	100.0% (84-100)	100.0% (40-100)	100.0% (84-100)	100.0% (86-100)	1	<0.001
TRUFI	4 (16.0%)	100.0% (40-100)	100.0% (84-100)	100.0% (40-100)	100.0% (84-100)	100.0% (86-100)	1	<0.001
STIR	4 (16.0%)	100.0% (40-100)	100.0% (84-100)	100.0% (40-100)	100.0% (84-100)	100.0% (86-100)	1	<0.001
Septal Thickening/Reticulations								
Overall	24 (96.0%)	100.0% (86-100)	100.0% (3-100)	100.0% (86-100)	100.0% (3-100)	100.0% (86-100)	1	<0.001
T2 HASTE	24 (96.0%)	100.0% (86-100)	100.0% (3-100)	100.0% (86-100)	100.0% (3-100)	100.0% (86-100)	1	<0.001
T2 BLADE	24 (96.0%)	100.0% (86-100)	100.0% (3-100)	100.0% (86-100)	100.0% (3-100)	100.0% (86-100)	1	<0.001
T1 VIBE	24 (96.0%)	100.0% (86-100)	100.0% (3-100)	100.0% (86-100)	100.0% (3-100)	100.0% (86-100)	1	<0.001
TRUFI	18 (72.0%)	75.0% (53-90)	100.0% (3-100)	100.0% (81-100)	14.3% (0-58)	76.0% (55-91)	0.19	0.102
STIR	24 (96.0%)	100.0% (86-100)	100.0% (3-100)	100.0% (86-100)	100.0% (3-100)	100.0% (86-100)	1	<0.001
Bronchial dilatation and subpleural multicystic changes								
Overall	14 (56.0%)	88.9% (68-100)	100.0% (29-100)	100.0% (84-100)	81.8% (19-99)	92.6% (80-100)	0.84	0.001
T2 HASTE	11 (44.0%)	76.2% (55-97)	100.0% (29-100)	100.0% (82-100)	64.3% (12-88)	83.3% (66-97)	0.6	0.001
T2 BLADE	14 (56.0%)	88.9% (68-100)	100.0% (29-100)	100.0% (84-100)	81.8% (19-99)	92.6% (80-100)	0.84	0.001
T1 VIBE	14 (56.0%)	88.9% (68-100)	100.0% (29-100)	100.0% (84-100)	81.8% (19-99)	92.6% (80-100)	0.84	0.001
TRUFI	3 (12.0%)	13.6% (3-35)	100.0% (29-100)	100.0% (29-100)	13.6% (3-35)	24.0% (9-45)	0.04	0.495
STIR	3 (12.0%)	13.6% (3-35)	100.0% (29-100)	100.0% (29-100)	13.6% (3-35)	24.0% (9-45)	0.04	0.495
Parenchymal Bands								
Overall	13 (52.0%)	92.9% (66-100)	100.0% (72-100)	100.0% (75-100)	91.7% (62-100)	96.0% (80-100)	0.92	<0.001
T2 HASTE	13 (52.0%)	92.9% (66-100)	100.0% (72-100)	100.0% (75-100)	91.7% (62-100)	96.0% (80-100)	0.92	<0.001
T2 BLADE	13 (52.0%)	92.9% (66-100)	100.0% (72-100)	100.0% (75-100)	91.7% (62-100)	96.0% (80-100)	0.92	<0.001
T1 VIBE	13 (52.0%)	92.9% (66-100)	100.0% (72-100)	100.0% (75-100)	91.7% (62-100)	96.0% (80-100)	0.92	<0.001
TRUFI	12 (48.0%)	85.7% (57-98)	100.0% (72-100)	100.0% (74-100)	84.6% (55-98)	92.0% (74-99)	0.84	<0.001
STIR	13 (52.0%)	92.9% (66-100)	100.0% (72-100)	100.0% (75-100)	91.7% (62-100)	96.0% (80-100)	0.92	<0.001
Crazy paving								
Overall	4 (16.0%)	100.0% (40-100)	100.0% (84-100)	100.0% (40-100)	100.0% (84-100)	100.0% (86-100)	1	<0.001
T2 HASTE	4 (16.0%)	100.0% (40-100)	100.0% (84-100)	100.0% (40-100)	100.0% (84-100)	100.0% (86-100)	1	<0.001
T2 BLADE	4 (16.0%)	100.0% (40-100)	100.0% (84-100)	100.0% (40-100)	100.0% (84-100)	100.0% (86-100)	1	<0.001
T1 VIBE	4 (16.0%)	100.0% (40-100)	100.0% (84-100)	100.0% (40-100)	100.0% (84-100)	100.0% (86-100)	1	<0.001
TRUFI	1 (4.0%)	25.0% (1-81)	100.0% (84-100)	100.0% (3-100)	87.5% (68-97)	88.0% (69-97)	0.36	0.019
STIR	2 (8.0%)	50.0% (7-93)	100.0% (84-100)	100.0% (16-100)	91.3% (72-99)	92.0% (74-99)	0.63	<0.001
Pleural thickening								
Overall	8 (32.0%)	100.0% (63-100)	100.0% (80-100)	100.0% (63-100)	100.0% (80-100)	100.0% (86-100)	1	<0.001
T2 HASTE	8 (32.0%)	100.0% (63-100)	100.0% (80-100)	100.0% (63-100)	100.0% (80-100)	100.0% (86-100)	1	<0.001
T2 BLADE	8 (32.0%)	100.0% (63-100)	100.0% (80-100)	100.0% (63-100)	100.0% (80-100)	100.0% (86-100)	1	<0.001
T1 VIBE	8 (32.0%)	100.0% (63-100)	100.0% (80-100)	100.0% (63-100)	100.0% (80-100)	100.0% (86-100)	1	<0.001
TRUFI	7 (28.0%)	87.5% (47-100)	100.0% (80-100)	100.0% (59-100)	94.4% (73-100)	96.0% (80-100)	0.9	<0.001
STIR	8 (32.0%)	100.0% (63-100)	100.0% (80-100)	100.0% (63-100)	100.0% (80-100)	100.0% (86-100)	1	<0.001

BLADE, proprietary name for periodically rotated overlapping parallel lines with enhanced reconstruction [PROPELLER]; GGOs, ground glass opacities; HASTE, Half-fourier acquisition single-shot Turbo Spin-Echo; NPV, negative predictive value; PPV, positive predictive value; SpO_2, saturation of peripheral oxygen; STIR, short tau inversion recovery; TRUFI, true fast imaging with steady state free precession; VIBE, volume interpolated breath-hold examination.

88.9% (95% CI, 68-100) sensitivity, and 100% (95% CI, 29-100) specificity (Fig 5). On T2 HASTE, 11/25 (44%) subjects showed bronchial dilatation/subpleural multicystic changes with sensitivity of 76.2% (95% CI, 55-97), and specificity of 100% (95% CI, 29-100). The sensitivity for TRUFI and STIR sequences for detection of bronchial dilatation/subpleural multicystic changes was 13.6 % (95% CI, 3-35) and specificity of 100% (95% CI, 29-100). The parenchymal bands (n=13/25, 52%) and pleural thickening (n=8/25, 32%) were detected with 100% sensitivity (95% CI, 40-100) and 100% specificity (95% CI, 84-100) on T2 HASTE, T2 BLADE, T1 VIBE, and STIR sequences (Fig 6). TRUFI has 85.7% (57-98) sensitivity for parenchymal bands and 87% sensitivity (95% CI, 47-100) for pleural thickening, with 100% specificity for both the findings.

Consolidation was found in 4/25 (16%) of subjects with 100% sensitivity (95% CI, 40-100) and 100% specificity (95% CI, 84-100) on all sequences, including T2 HASTE, T2 BLADE, T1 VIBE, TRUFI, and STIR. Crazy-paving was seen in 4/25 (16%) of subjects with 100% (CI 95%, 40%-100%) sensitivity and 100% (95% CI, 84-100) specificity on T2 HASTE, T2 BLADE, and T1 VIBE sequences. STIR and TRUFI sequences were 50% (95% CI, 7-93) and 25% (95% CI, 1- 81) sensitive for detection of crazy-paving, respectively, with 100% specificity.

In a nutshell, on overall analysis, almost perfect agreement (k=0.8-1, P-value <0.05) was noted between CT chest and MRI chest findings. The overall sensitivity and specificity of MRI chest for detecting GGOs, consolidation, septal thickening and reticulations, pleural thickening, and crazy-paving was 100%; while the sensitivity for parenchymal bands and bronchial dilatation/subpleural multicystic changes was 92.9% and 88.9% respectively, with specificity of 100% for both.

DISCUSSION

Our study aimed to determine the accuracy of MRI chest and its various sequences in evaluating the pulmonary sequelae of patients recovered from COVID-19 ARDS, with no such study published in the literature to date to the best of our knowledge. The present study

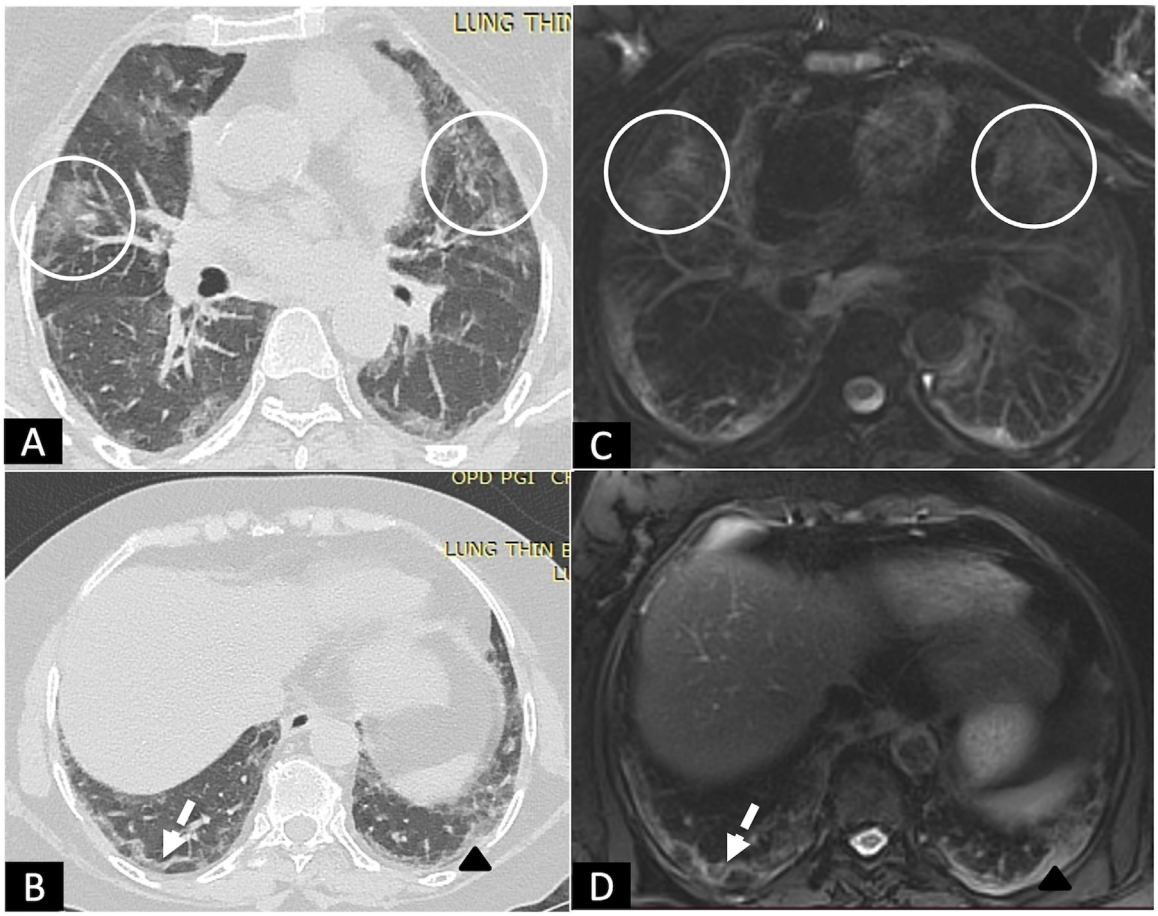

FIG 2. A 53-year female following recovery from post COVID-19 ARDS, with complaints of mild exertional dyspnea at 6 weeks. (A,B), HRCT chest and (C,D), corresponding MRI T2 BLADE images showing peripheral subpleural curvilinear bands with arcade-like sign (white dashed arrows) and patchy areas of ground glass opacities (circles) in bilateral lungs, with few areas of irregular pleural thickening (black arrowheads) on left side. (Color version of figure is available online.)

revealed that the MRI chest has the ability to reliably delineate the radiological abnormalities of post-COVID lung when compared to the gold standard CT chest. We found the commonly encountered imaging findings at 6 weeks' follow-up of COVID-19 pneumonia were GGOs, interstitial thickening and reticulations, bronchial dilatation/subpleural multicystic changes, parenchymal bands, consolidation, and crazy-paving; and these were detected both by MRI and CT with almost perfect agreement (k=0.8-1).

Overall, we found that T2 BLADE and T1 VIBE sequences are 100% specific and greater than 93% sensitive for detecting GGOs, septal thickening/reticulations, parenchymal bands, consolidation, and crazy-paving appearance with 95% CI. Bronchial dilatation and parenchymal bands were missed in few patients on MRI chest when compared to CT. This is in coherence with the prospective 2-center study on subjects with cystic fibrosis by Ciet P et al., who reported low sensitivity 0.33 (CI 0.09-0.57) of MRI chest in the detection of bronchiectasis when compared to CT.[19] The poor ability of MRI to detect trapped air is thought to be the cause for false-negative results in the detection of bronchiectasis. Moreover, in general, MRI is considered relatively less sensitive for the detection of air compared to CT.[19]

There was 100% sensitivity and 100% specificity for detection of GGOs, septal thickening/reticulations, and pleural thickening on MRI chest with a perfect agreement (k=1) between the CT and MRI. However, a prospective study from Italy on post-COVID subjects after discharge reported more GGOs and interstitial thickening on MRI than CT with the reported frequency of 94.2% vs 76.9%, and 86.5% vs 78.8%, for MRI chest and CT chest, respectively.[13] The sensitivity and specificity for GGOs on the MRI chest were 100% (95% CI: 0.91-1.00) and

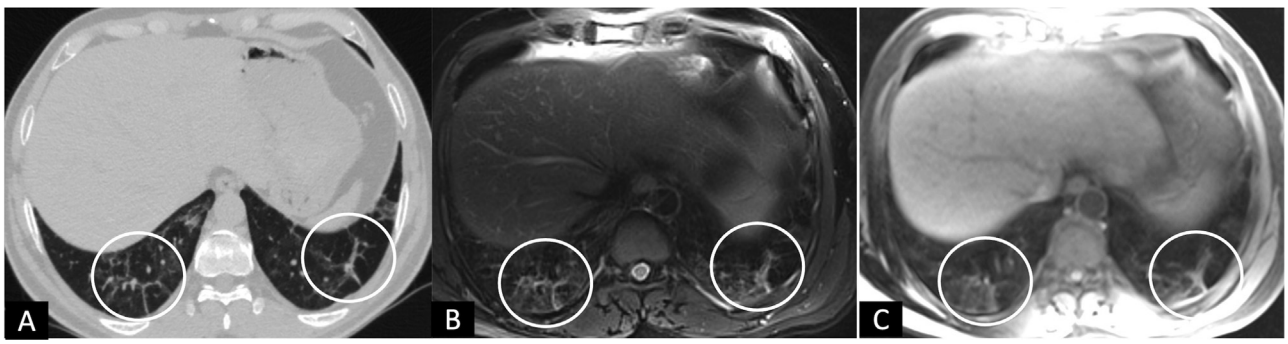

FIG 3. A 46-years-old male with complaint of MMRC grade-II dyspnea 6 weeks after discharge. (A), HRCT chest, and (B, C), corresponding axial MRI T2 BLADE and T1 VIBE images showing areas of septal thickening (circles).

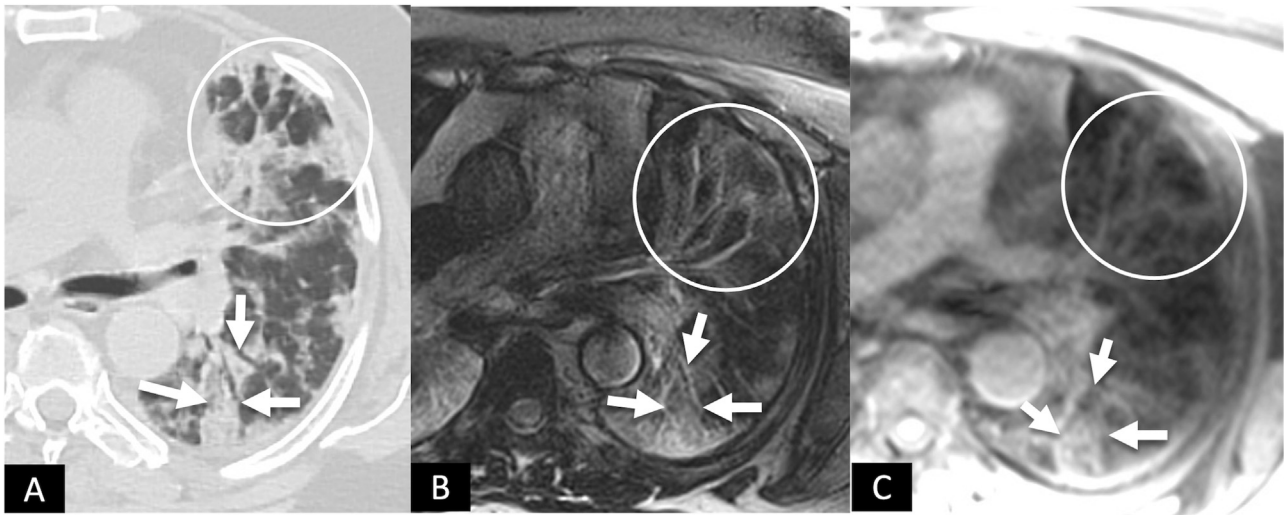

FIG 4. A 60-year-old male with complaints of shortness of breath and fatigue at 6 weeks following recovery from post-COVID-19 ARDS. (A), HRCT chest and corresponding axial MRI images (B), T2 BLADE and (C), T1 VIBE showing patchy areas of consolidation (white solid arrows) in the superior segment of left lower lobe. Also note the patchy areas of GGOs interspersed with reticulations anteriorly (circles). (Color version of figure is available online.)

25% (95% CI: 0.05-0.57), respectively. Additionally, the same study also reported the highest sensitivity for detection of interstitial thickening on MRI chest (1.00, 95% CI: 0.91-1.00), but with low specificity (0.64, 95% CI: 0.31-0.89).[11] Another prospective study on HIV children reported moderate sensitivity and high specificity of the MRI chest for detection of GGOs with values of 75% (95% CI: 34.9%-96.8%) and 94.1% (95%: 71.3%-99.9%), respectively.[20]

The variation in the reported sensitivity and specificity in different studies may result from different sequences employed to evaluate

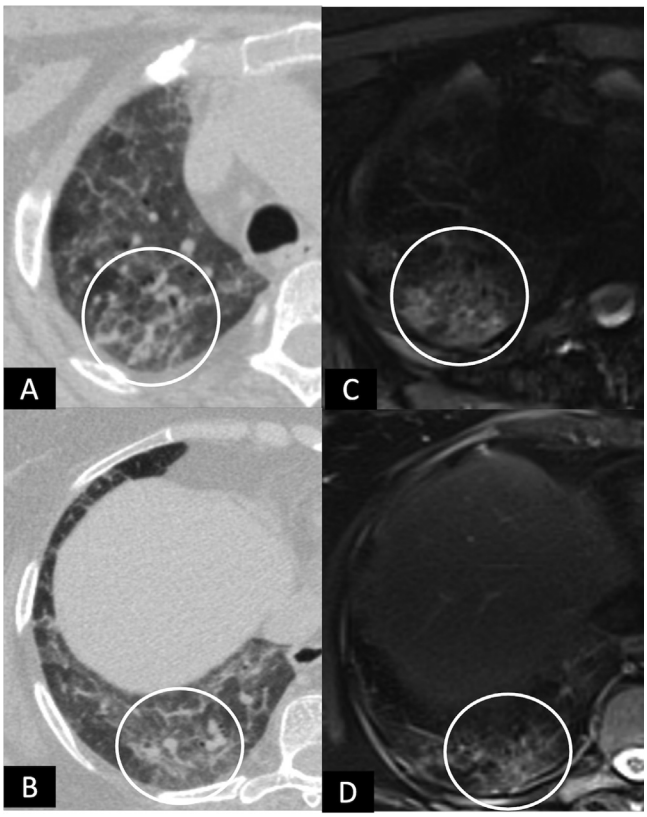

FIG 5. A 49-years-old female with complaint of MMRC grade-III dyspnea 6 weeks after discharge. (A,B), HRCT chest and (C,D), MRI T2 BLADE images showing areas of ground glass opacities and septal thickening giving crazy paving pattern (white circles) in right lung, at 2 different levels in right upper and lower lobes.

the pulmonary findings. We found T2 HASTE, T2 BLADE, T1 VIBE, and STIR sequences detecting 100% of subjects with GGOs and interstitial thickening. TRUFI could detect only 75% of interstitial thickening and 80% GGOs. Pecoraro et al. reported false-positive results for GGOs in 9 subjects on MRI chest, and the authors claimed the superior role of MRI with its ability to discriminate the GGOs by quantifying the proton density of alveolar contents.[13] Nevertheless, CT has a high spatial resolution as compared to MRI,[20] and no other studies comparing CT and MRI chest imaging reported higher detection of GGOs on MRI than CT. Rana et al. reported false-positive detection of GGOs on T2-W TSE, T2-W MultiVane XD and T1W mDixon sequences in 1 child; and on SSFP sequence in 2 subjects.[21]

Bronchial dilatation/subpleural multicystic change was the next common finding seen on CT chest in 64% (16/25) subjects of our cohort, with reported sensitivity and specificity of 88.9% (95% CI: 68-100) and 100.0% (CI: 29-100) for thoracic MRI, respectively. In contrast to our findings, Pecoraro et al. has reported subpleural multicystic changes in one-third 36.5% (19/52) of subjects on CT chest, and none on MRI.[11] This can be attributed to the different demographic and clinical strata of the 2 study cohorts. We included a cohort of subjects with COVID-19 ARDS and did follow-up imaging at 6 weeks from hospital discharge. The clinical status of the cohort included by Percoraro et al. was heterogeneous and consisted of participants with variable clinical severity ranging from mild to severe disease, and that could have resulted in a lesser fraction of subjects with subpleural multicystic changes. Early scheduling of follow-up CT and MRI chest (~11 days following remission (RT-PCR negative), IQR: 11.25-23 days) by Pecoraro and colleagues may be another reason for the low detection rate of subpleural multicystic changes. Moreover, Percoraro et al. mentioned in their study that non-addition of 3D T1 sequences into their acquisition protocol might have resulted in a poor agreement between CT and MRI findings.[13] Nevertheless, we could detect bronchial dilatation in 14/16 of our subjects on T1 VIBE and T2 BLADE sequences. The presence of diffuse GGOs and other interstitial changes in our study cohort due to ARDS might have contributed in enhancing the background contrast of lung parenchyma, making the areas of bronchial dilatation conspicuous for detection. In another study, Rana et al. reported the sensitivity to detect bronchiectasis was 75% (42.8%–94.5%), 81.8% (48.2%-97.7%), and 27.3% (6.0%-60.9%) for T2W TSE, T2W MultiVane XD and SSFP sequences, respectively.[21]

Parenchymal bands are found in more than half (14/25) of the subjects in our study on CT chest and 13 subjects on MRI. The T2

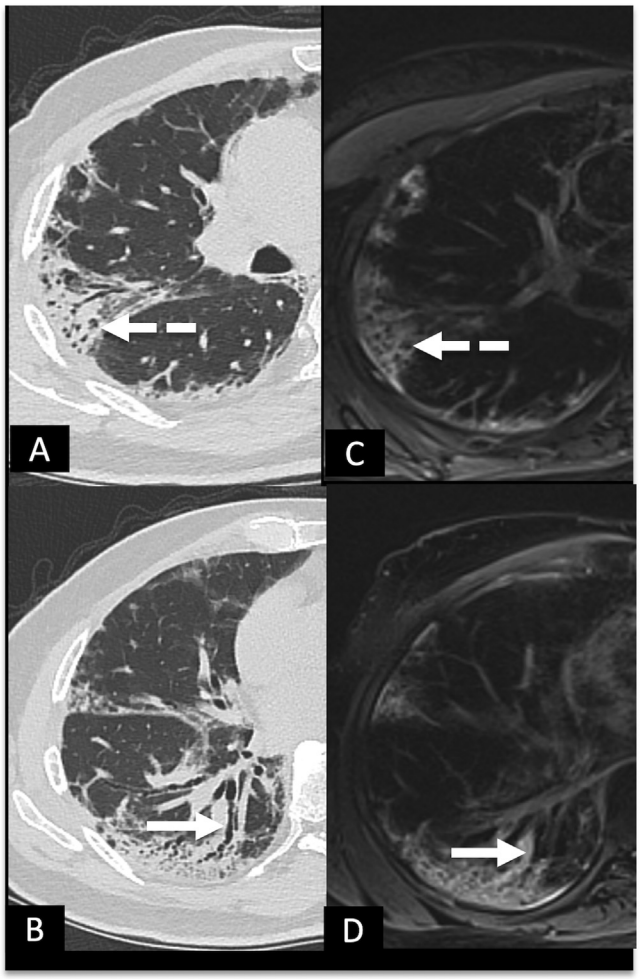

FIG 6. A 61-year-old male with complaints of cough and expectoration following COVID-19 ARDS. (A,B), HRCT chest and corresponding MRI T2 BLADE images (C,D), showing bronchial dilatation (white solid arrows) and subpleural multicystic changes (white dashed arrows). (Color version of figure is available online.)

HASTE, T2 BLADE, T1 VIBE, and STIR sequences have similarly detected 13 subjects with parenchymal bands; while no comparative details are available in the study published by Percoraro et al.[11] Consolidation and crazy-paving, each found in 4 (16%) subjects in our cohort with a perfect agreement between CT and MRI findings. Percoraro et al. also reported 100% agreement between CT and MRI modalities, while in another study, Sodhi et al. reported 100% agreement between the CT and MRI findings in children with consolidation (non-COVID).[13,22] We found a similar rate of detection on all the MRI sequences we utilized in our study. Other studies also report a 100% detection rate for consolidation/collapse on MRI irrespective of the sequences used.[13,21-23]

Being a radiation-free modality, the MRI chest has been increasingly used in the recent past for the evaluation of various lung disorders. There is much scope for further improvement of lung MRI in the evaluation of the post-COVID lungs in the future, especially to explore the utility of functional MRI (Hyperpolarized xenon [129Xe] MRI, contrast-enhanced MRI, oxygen-enhanced proton MRI and DW [diffusion-weighted] MRI) to provide the holistic approach in subjects with post-COVID pulmonary sequel, including diffusion alterations and activity of the pulmonary lesions.[24,25] This might impact the treatment decisions and assist in patient management. Our study highlights the use of routine T1 and T2 sequences for accurate detection of pulmonary findings, and it may also act as a shred of preliminary evidence for further advancement in MRI research in post-COVID pulmonary manifestations.

However, there are few limitations in our study. Our sample size is small and we included only COVID-19 ARDS recovered patients, which may not reflect the true incidence of lung abnormalities recognized on the MRI chest. However, it is noteworthy that our observations remained consistent among all the patients. Secondly, we used only the basic MRI sequences, while the newer MR sequences like ultrashort TE (UTE) and zero TE proton MRI could have provided even better image quality.[25] Thirdly, we could not run functional MRI sequences, which could have aided in differentiating active/inflammatory versus inactive/fibrotic lesions, thus limiting our results and conclusions only to the structural changes seen on MRI chest. And lastly, we evaluated only the imaging patterns and didn't grade the extent of pulmonary involvement as seen on CT and MRI. Additionally, there is a possibility of bias as the radiologists who evaluated the studies knew beforehand that the recruited subjects are follow-up cases of COVID-19 related ARDS.

To conclude, MRI chest showed good agreement with CT chest in the evaluation of pulmonary sequel in patients recovered from COVID-19 pneumonia. Being a radiation-free modality, it has the potential to act as an alternate imaging tool to CT chest in the evaluation of post-COVID lungs; as these patients may require extensive longitudinal follow-up. However, there is a need for standardization and optimization of MRI sequences for pulmonary imaging; and further prospective and longitudinal studies among larger cohorts of patients are required to validate the diagnostic accuracy of MRI chest in the follow-up of COVID-19 pneumonia.

REFERENCES

1. Office for National Statistics. The prevalence of long COVID symptoms and COVID-19 complications. [updated December 16, 2020]. Available at: https://www.ons.gov.uk/.
2. Torres-Castro R, Vasconcello-Castillo L, Alsina-Restoy X, et al. Respiratory function in patients post-infection by COVID-19: a systematic review and meta-analysis. Pulmonology 2021;27:328–37, https://doi.org/10.1016/j.pulmoe.2020.10.013.
3. Han X, Fan Y, Alwalid O, et al. Six-month follow-up chest CT findings after severe COVID-19 Pneumonia. Radiology 2021;299(1):E177–86, https://doi.org/10.1148/radiol.2021203153.
4. Garg M, Maralakunte M, Garg S, et al. The conundrum of 'long-covid-19′: a narrative review. Int J Gen Med 2021;14:2491–506, https://doi.org/10.2147/IJGM.S316708.
5. Garg M, Prabhakar N, Bhalla AS, et al. Computed tomography chest in COVID-19: when & why? Indian J Med Res 2021;153:86–92, https://doi.org/10.4103/ijmr.IJMR_3669_20.
6. Garg M, Gupta P, Maralakunte M, et al. Diagnostic accuracy of CT and radiographic findings for novel coronavirus 2019 Pneumonia: systematic review and meta-analysis. Clin Imaging 2021;72:75–82, https://doi.org/10.1016/j.clinimag.2020.11.021.
7. Prabhakar N, Prabhakar A, Garg M. Chest CT in "post" COVID-19: what the radiologist must know. Radiographics 2021;41(2):E66–7, https://doi.org/10.1148/rg.2021200213.
8. Han X, Fan Y, Alwalid O, et al. Fibrotic interstitial lung abnormalities at 1-year follow-up CT after severe COVID-19. Radiology 2021:210972, https://doi.org/10.1148/radiol.2021210972.
9. George PM, Barratt SL, Condliffe R, et al. Respiratory follow-up of patients with COVID-19 Pneumonia. Thorax 2020;75(11):1009–16, https://doi.org/10.1136/thoraxjnl-2020-215314.
10. Vasilev YA, Sergunova KA, Bazhin AV, et al. Chest MRI of patients with COVID-19. MagnReson Imaging 2021;79:13–9, https://doi.org/10.1016/j.mri.2021.03.005.
11. Torkian P, Rajebi H, Zamani T, et al. Magnetic resonance imaging features of coronavirus disease 2019 (COVID-19) pneumonia: the first preliminary case series. Clin Imaging 2021;69:261–5, https://doi.org/10.1016/j.clinimag.2020.09.002.
12. Garg M, Prabhakar N, Dhooria S, et al. Magnetic resonance imaging (MRI) chest in post-COVID-19 pneumonia. Lung India 2021;38(5):498–9, https://doi.org/10.4103/lungindia.lungindia_206_21.
13. Pecoraro M, Cipollari S, Marchitelli L, et al. Cross-sectional analysis of follow-up chest MRI and chest CT scans in patients previously affected by COVID-19. Radiol Med 2021:1–9, https://doi.org/10.1007/s11547-021-01390-4.
14. Garg MK, Sharma M, Agarwal R, et al. Allergic Bronchopulmonary Aspergillosis: all a radiologist needs to know. CurrPediatr Rev 2016;12:179–89, https://doi.org/10.2174/1573396312666160831143951.
15. World Health Organization. Clinical management of severe acute respiratory infection when novel coronavirus (nCoV) infection is suspected: interim guidance. Available at: https://www.who.int/docs/default-source/coronaviruse/clinical-management-ofnovel-cov.pdf.

16. Definition Task Force ARDS, Ranieri VM, et al. Acute respiratory distress syndrome: the Berlin Definition. JAMA 2012;307:2526–33, https://doi.org/10.1001/jama.2012.5669.
17. European Centre for Disease Prevention and Control. Guidance for discharge and ending of isolation of people with COVID-19. Available at: https://www.ecdc.europa.eu/en/publications-data/covid-19-guidance-discharge-and-ending-isolation.
18. Hansell DM, Bankier AA, MacMahon H, et al. Fleischner society: glossary of terms for thoracic imaging. Radiology 2008;246(3):697–722, https://doi.org/10.1148/radiol.2462070712.
19. Ciet P, Serra G, Bertolo S, et al. Assessment of CF lung disease using motion corrected PROPELLER MRI: a comparison with CT. Eur Radiol 2016;26(3):780–7, https://doi.org/10.1007/s00330-015-3850-9.
20. Lin E, Alessio A. What are the basic concepts of temporal, contrast, and spatial resolution in cardiac CT? J Cardiovasc Comput Tomogr 2009;3(6):403–8, https://doi.org/10.1016/j.jcct.2009.07.003.
21. Rana P, Sodhi KS, Bhatia A, et al. Diagnostic accuracy of 3-T lung magnetic resonance imaging in human immunodeficiency virus-positive children. Pediatr Radiol 2020;50(1):38–45, https://doi.org/10.1007/s00247-019-04523-0.
22. Sodhi KS, Sharma M, Saxena AK, et al. MRI in thoracic Tuberculosis of children. Indian J Pediatr 2017;84(9):670–6, https://doi.org/10.1007/s12098-017-2392-3.
23. Sodhi KS, Sharma M, Lee EY, et al. Diagnostic utility of 3T lung MRI in children with interstitial lung disease: a prospective pilot study. AcadRadiol 2018;25:380–6, https://doi.org/10.1016/j.acra.2017.09.013.
24. Li H, Zhao X, Wang Y, et al. Damaged lung gas exchange function of discharged COVID-19 patients detected by hyperpolarized 129Xe MRI. Sci Adv 2021;7(1):eabc8180, https://doi.org/10.1126/sciadv.abc8180.
25. Hatabu H, Ohno Y, Gefter WB, et al. Expanding applications of pulmonary MRI in the clinical evaluation of lung disorders: fleischner society position paper. Radiology 2020;297:286–301, https://doi.org/10.1148/radiol.2020201138.